



HHS Public Access

Author manuscript

Chemistry. Author manuscript; available in PMC 2022 January 26.

Published in final edited form as:

Chemistry. 2021 January 26; 27(6): 1990–1994. doi:10.1002/chem.202004389.

The photosensitizing efficacy of micelles containing a porphyrinic photosensitizer and KI against resistant melanoma cells

Kelly A. D. F. Castro^{a,b}, Letícia D. Costa^b, Juliana A. Prandini^a, Juliana C. Biazotto^a, Augusto C. Tomé^b, Michael R. Hamblin^{c,d}, Maria da Graça P. M. S. Neves^b, M. Amparo F. Faustino^b, Roberto S. da Silva^a

^[a]Department of Physics and Chemistry, Faculty of Pharmaceutical Sciences of Ribeirão Preto, University of São Paulo, Ribeirão Preto, São Paulo, Brazil

^[b]LAQV-REQUIMTE, Department of Chemistry, University of Aveiro, Aveiro, Portugal

^[c]Wellman Center for Photomedicine, Massachusetts General Hospital, Harvard Medical School, Boston, MA 02114, USA

^[d]Laser Research Centre, Faculty of Health Science, University of Johannesburg, Doornfontein 2028, South Africa

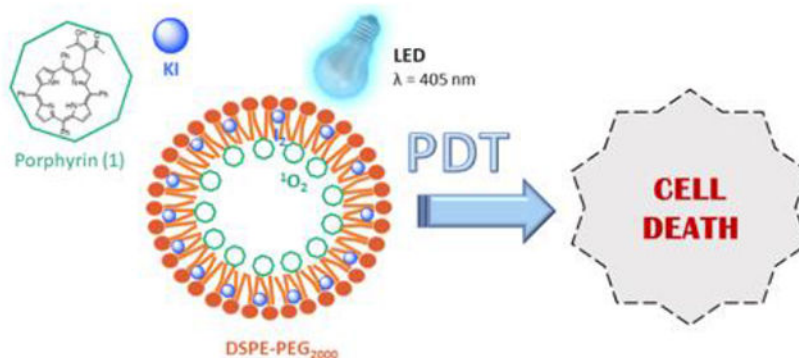
Abstract

Photodynamic therapy (PDT) appears as a promising alternative to overcome the resistance of melanoma to conventional therapies. Currently applied photosensitizers (PS) are often based on tetrapyrrolic macrocycles like porphyrins. Unfortunately, in some cases the use of this type of derivatives is limited due to their poor solubility in the biological environment. Feasible approaches to surpass this drawback are based on lipid formulations. Besides that, and inspired in the efficacy of potassium iodide (KI) for antimicrobial photodynamic therapy (aPDT), the combined effect of ¹O₂ with KI was assessed in this work, as an alternative strategy to potentiate the effect of PDT against resistant melanoma cells.

Graphical Abstract

silva@usp.br.

Supporting information for this article is given via a link at the end of the document.



To overcome the poor solubility of porphyrins in biological systems, in this communication we propose the simultaneous encapsulation of a porphyrinic photosensitizer and KI into a lipid-based drug delivery system. After prepared and duly characterized, these micelles were used in the photodynamic treatment of melanoma cells. As expected, the photodynamic efficacy increases as the concentration of both porphyrin and KI encapsulated also increases.

Keywords

porphyrin; melanoma; PDT; singlet oxygen; iodine

Porphyrin derivatives have been widely used as photosensitizing agents against tumoral cells or microorganisms.^[1] Their therapeutic action is based on the production of reactive oxygen species (ROS) upon visible light irradiation^[2] in a modality called photodynamic therapy (PDT). Beyond the requirement of ROS production, the efficiency of those compounds is strictly dependent on their uptake by the target cells, which in turn is mainly determined by molecular structure and solubility of these PS in the biological medium. So, despite the aforementioned advantages of porphyrins, certain negative features involving their biological action as photosensitizers have been reported.^[1a, g] Indeed, the dependence on the PS photocytotoxicity with its subcellular localization has been pointed out as the main limiting factor, since the cellular damage is confined to the area where the ROS are produced and these species have a limited diffusion distance in the biological media.^[3] Although PDT was already approved by the US Food and Drug Administration (FDA) and European agencies to treat some oncological and pre-oncological diseases (*e.g.*, non-melanoma skin cancers (NMSC) and actinic keratosis, as successful examples of the use of PDT to treat skin diseases),^[4] their efficiency to treat melanoma is still limited and needs to be improved.^[4d, e, 5] Actually, the melanotic melanomas are much less responsive to the treatment than the amelanotic ones.^[6] In fact, it is well known that melanin plays an important role in the photoprotection of skin by absorbing the UV radiation. Briefly, beyond compete with the PS for light absorption (around *ca.* 500–600 nm), melanin also acts as antioxidant, thereby decreasing the levels of ROS and enable cell survival and proliferation.^[6a, b, f, 7] In the last years, several strategies have been studied to overcome the resistance of melanoma.^[8] Noteworthy, almost all of these approaches, that aim at the melanosome disruption to block the production of melanin, involve the use of targeted or combined therapies.^[8] By assuming that it is fundamental to overcome the tolerance of these cells to the oxidative

stress^[6b, 7] in this work we adopted a strategy that has been applied with great success in the antimicrobial photodynamic therapy (aPDT). This approach relies in the increased production of reactive species through the combination of $^1\text{O}_2$ and potassium iodide (KI), aiming that the free iodine (I_2/I_3^-) and reactive iodine radicals ($\text{I}_2^\bullet/\text{I}^\bullet$) thereby produced could enhance the killing of cancer cells.^[9] Indeed, potassium iodide is a well-known anti-inflammatory drug, whose dermatological application at established doses is already described in the literature.^[10] To the best of our knowledge, this is the first report about the combined action of these two species against cancer cells, and in particular against the B16F10 melanoma cell line. Moreover, the PS and KI were encapsulated into micelles in order to avoid the constrains that usually occur due to the low solubility of the PS in biological media, thereby ensuring that the PS was uptaken by the target cells in the monomeric form.

Porphyrin (**1**) was prepared and characterized by $^1\text{H-NMR}$ and UV-Vis spectroscopy (Figure 1 and Supplementary material: Figures S1–S3). The analytical results are in full agreement with the literature.^[11] Porphyrin (**1**) has a poor solubility in aqueous media and therefore a great trend to aggregate (Figure S4). Therefore, its encapsulation in a lipid-based nanosized carrier aims to increase their solubility and dispersion in the biological environment. Described by some of us several years ago,^[11a] this porphyrin has anchoring groups that enable an efficient loading into the DSPE-PEG micelles.^[12] Although porphyrins are recognized as good producers of $^1\text{O}_2$, not always they are able to trigger a cytotoxic response against some types of cancer cells as one would expect from a phototherapeutic agent. Thus, combinational therapies represent an advantageous strategy to enhance the treatment efficiency thereby allowing even the treatment of resistant cancers.

Take it into account, we propose the use of a porphyrin in combination with KI to treat melanoma cancer. Notwithstanding no studies have been done to determine the exact location of both porphyrin (**1**) and KI into this lipidic formulation, the lipid **DSPE-PEG** contain non-polar groups that are responsible for a strong interaction with hydrophobic porphyrins,^[13] and allows their incorporation in the micelles core. In turn, the hydrophilic KI interacts with the polymeric structure of PEG chains,^[14] and we therefore believe that it is probably located there.

The lipid formulations (**1-DSPE-PEG**) and (**1-DSPE-PEG/KI**), prepared with porphyrin (**1**) in the absence and in the presence of KI, respectively, have a zeta potential of *ca.* -30 mV and an average size smaller than 100 nm (PdI ~ 0.29) (see SI Figs. S5–S12). Similar results were obtained for the control formulations (**DSPE-PEG**) and (**DSPE-PEG/KI**), prepared without porphyrin. As expected, these lipid formulations improve the solubility of (**1**) in biological media. The presence of KI had no influence on the porphyrin solubility (Figure 2). Regarding the spectral features of these lipid formulations, the incorporation of porphyrin (**1**) is confirmed by the presence of the Soret and Q bands characteristic of porphyrin derivatives in both formulations without (**1-DSPE-PEG**) or with KI (**1-DSPE-PEG/KI**). Beyond that, the (**1-DSPE-PEG/KI**) has an additional band at 230 nm, which was attributed to the interaction of (**1**) with the KI present in the lipid formulation. The emission spectra obtained for both formulations after excitation at *ca.* 420 nm present the two characteristic

bands of porphyrin derivatives, the Q(0,0) and Q(0,1), centered at *ca.* 656 and 726 nm, respectively.

The excitation spectra were also acquired and are perfectly overlapped on the corresponding absorption spectra (Figure 2). The effect of blue light on **(1)**, **(1-DSPE-PEG)** and **(1-DSPE-PEG/KI)** was evaluated by UV-visible and fluorescence spectroscopies. In general, a decrease of 24% in the Soret band absorbance was observed for porphyrin **(1)** after 5 min of blue light irradiation (405 nm) (Figure S13). This behaviour may be associated to photodegradation and/or to aggregation phenomena.^[15] For the formulation **(1-DSPE-PEG)**, a comparable decrease of 26% in the Soret band was only observed after 60 min of irradiation (Figure S14). The remarkable photostability of **(1)** provided by the lipidic microenvironment is not observable in aqueous solution. In turn, the irradiation of the formulation **(1-DSPE-PEG/KI)** with blue light leads to the appearance of a new species with a Soret centered at 437 nm, and whose presence is clearly evident in the UV-Vis spectra acquired during the irradiation experiment (Figure 3). The formation of this species is concomitant with the decrease of porphyrin **(1)** Soret band at 422 nm. The well-defined isosbestic point at 430 nm seems to indicate a simple photochemical reaction that it is being favoured by the presence of KI. Analogously, the Q-bands were also significantly affected as a function of the irradiation time (Figure 3B). The widening of the Q-bands may reflect a change in the porphyrin molecular environment due to the presence of KI, which apparently results in a distortion from planarity or in an extension of the skeleton conjugation. Noteworthy, the formation of new species is also evident by the appearance of a new band at 676 nm (Figure 3B). The fluorescence spectra of the irradiated solution of **(1-DSPE-PEG/KI)** (Figure 4 and Figure S15) also confirms the formation of a new species since the intensity of the emission band at 656 nm decreases with the concomitant increase of a new band at 680 nm during the irradiation time, which is in full accordance with the new band observed in the corresponding absorption spectrum (Figures 3 and 4). In the assays performed under blue-light irradiation with porphyrin **(1)** dissolved in an aqueous solution of DMSO (1%) and containing KI, the appearance of two bands at *ca.* 289 and 356 nm, whose intensity was dependent on the irradiation time, supports the production of I₂ (Supplementary material: Figure S13).^[9d] The formation of I₂ is triggered by the oxidation of the iodide anion by the singlet oxygen produced during the light irradiation of the porphyrin **(1)**. The referred bands are characteristic of tri-iodide (I₃⁻).^[15c]

Porphyrin **(1)** and the lipid-porphyrin formulations **(1-DSPE-PEG)** and **(1-DSPE-PEG/KI)** at PS concentrations between 0.5-20 μM were used in cytotoxicity assays against B16F10 cells as a melanoma model. Dose-dependent cytotoxicity is showed in Figure 5. The results obtained with porphyrin **(1)** at concentrations between 0.5-20 μM with KI or by the lipid formulations in the absence or in the presence KI are summarized in Figure 5A and Figure S16 in SI.

The treatment of B16F10 cells with porphyrin **(1)** shows no cytotoxic effect either under dark (Figure S16) or light conditions (Figure 5A) for the tested concentrations. Similarly, when **(1)** and KI were combined in solution, the cell viability remained unaffected even after light irradiation (Figure 5A). However, lipid formulations of **(1-DSPE-PEG)** and **(1-DSPE-PEG/KI)** lead to different results. In dark conditions, both lipid formulations did not show

in vitro cytotoxicity to melanoma cells (Figure S16). In turn, the cell viability after blue light irradiation was dependent on the concentration of **(1)** in the micelles (Figure 5B). These data are in full agreement with the literature, that clearly evidences that the encapsulation of porphyrin derivatives in micelles improve the aPDT efficacy.^[1g, 16]

At low concentrations (0.5 μM), the photodynamic effect seems to be exclusively mediated by ROS, probably due to the non-significant amount of KI within the formulation. In fact, it must be stressed that there are several studies that demonstrate that the killing potentiation by addition of KI is only effective and statistically significant above a certain concentration, below which it has no effect.^[9d, 17] Increasing concentrations of porphyrin **(1)** (10 or 20 μM) also correspond to higher doses of KI (100 and 200 μM , respectively). So, the enhanced photodynamic effect clearly suggests the combined action of the singlet oxygen thereby generated with the iodine. The strong cytotoxic effect observed for **(1-DSPE-PEG)** and **(1-DSPE-PEG/KI)** could be attributed to non-aggregate state of porphyrin **(1)** during the PDT assays. Moreover, it may also be due to the cellular uptake improved by the lipid formulation, which enables a better interaction of the porphyrin with the hydrophilic portion of the lipid bilayer. Figure 6 shows the fluorescence microscopy images of **(1-DSPE-PEG)** and **(1-DSPE-PEG/KI)** in B16F10 cells. No fluorescence images could be obtained for the free porphyrin **(1)** due to the formation of aggregates.

In this work, it was found that lipid formulations containing porphyrin **(1)** or porphyrin **(1)** and KI can act as efficient photosensitizing agents against melanotic cancer cells. The use of a lipid-based drug delivery system allowed to overcome the poor solubility of porphyrin **(1)**, and consequently its aggregation in biological media, thereby contributing to its increased photocytotoxic action against B16F10 cells. Noteworthy, the combined effect of singlet oxygen and iodine, successfully applied on the antimicrobial PDT context, is here reported for the first time as a promising approach to treat resistant melanoma cells. The intrinsic fluorescence of porphyrin **(1)** allowed the monitorization of its cellular uptake.

Supplementary Material

Refer to Web version on PubMed Central for supplementary material.

Acknowledgements

Thanks are due to Conselho Nacional de Desenvolvimento Científico e Tecnológico (CNPq), Coordenação de Aperfeiçoamento de Pessoal de Nível Superior (CAPES), Fundação de Amparo à Pesquisa do Estado de São Paulo (FAPESP- 2016/12707-0), Universidade de São Paulo. We also thank the Fundação para a Ciência e a Tecnologia (FCT) for the financial support to the project PTDC/REQ-QOR/6160/2014, the QOPNA research unit (FCT UID/QUI/00062/2019) and the LAQV-REQUIMTE (UIDB/50006/2020) through national funds and, when applicable, co-financed by FEDER within the PT2020 Partnership Agreement. K.A.D.F. Castro thanks CAPES for the post-doctoral scholarship granted (PNPD/CAPES). L.D. Costa thanks FCT for the doctoral grant SFRH/PD/BD/114578/2016. MRH was supported by US NIH Grants R01AI050875 and R21AI121700.

References

- [1]. a) Kou J, Dou D and Yang L, *Oncotarget* 2017, 8, 81591–81603; [PubMed: 29113417] b) Malatesti N, Munitic I and Jurak I, *Biophys. Rev* 2017, 9, 149–168; [PubMed: 28510089] c) Zhang J, Jiang C, Figueiro Longo JP, Azevedo RB, Zhang H and Muehlmann LA, *Acta Pharm. Sin. B* 2018, 8, 137–146; [PubMed: 29719775] d) Ethirajan M, Chen Y, Joshi P and Pandey RK,

- Chem. Soc. Rev 2011, 40, 340–362; [PubMed: 20694259] e) Stojiljkovic I, Evavold BD and Kumar V, Expert Opin. Investig. Drugs 2001, 10, 309–320; f) Mesquita MQ, Dias CJ, Gamelas S, Fardilha M, Neves MGPMS and Faustino MAF, An. Acad. Bras. Cienc 2018, 90, 1101–1130; [PubMed: 29873674] g) Mesquita MQ, Dias CJ, Neves MGPMS, Almeida A and Faustino MAF, Molecules 2018, 23, 1–47.
- [2]. a) Clemente N, Miletto I, Gianotti E, Invernizzi M, Marchese L, Dianzani U and Renò F, J. Photochem. Photobiol. B 2019, 197, 111533; [PubMed: 31254952] b) Allison RR and Moghissi K, Clin. Endosc 2013, 46, 24–29; [PubMed: 23422955] c) Castano AP, Demidova TN and Hamblin MR, Photodiagn. Photodyn 2004, 1, 279–293; d) Abrahamse H and Hamblin MR, Biochem. J 2016, 473, 347–364. [PubMed: 26862179]
- [3]. a) Wang H and Fei B, J Magn Reson Imaging 2010, 32, 409–417; [PubMed: 20677270] b) O'Connor AE, Gallagher WM and Byrne AT, Photochem. Photobiol 2009, 85, 1053–1074; [PubMed: 19682322] c) Ormond AB and Freeman HS, Materials (Basel) 2013, 6, 817–840 [PubMed: 28809342]
- [4]. a) van Straten D, Mashayekhi V, de Bruijn HS, Oliveira S and Robinson DJ, Cancers (Basel) 2017, 9; b) Agostinis P, Berg K, Cengel KA, Foster TH, Girotti AW, Gollnick SO, Hahn SM, Hamblin MR, Juzeniene A, Kessel D, Korbelik M, Moan J, Mroz P, Nowis D, Piette J, Wilson BC and Golab J, CA Cancer J. Clin 2011, 61, 250–281; [PubMed: 21617154] c) Dougherty TJ, Gomer CJ, Henderson BW, Jori G, Kessel D, Korbelik M, Moan J and Peng Q, J. Natl. Cancer Inst 1998, 90, 889–905; [PubMed: 9637138] d) Triesscheijn M, Baas P, Schellens JH and Stewart FA, Oncologist 2006, 11, 1034–1044; [PubMed: 17030646] e) Gold MH, J Clin. Aesthet. Dermatol 2009, 2, 44–47.
- [5]. Naidoo C, Kruger CA and Abrahamse H, Technol. Cancer Res. Treat 2018, 17, 1533033818791795. [PubMed: 30099929]
- [6]. a) Baldea I and Filip AG, J. Physiol. Pharmacol 2012, 63, 109–118; [PubMed: 22653896] b) Bsaldea I, Giurgiu L, Teacoe ID, Olteanu DE, Olteanu FC, Clichici S and Filip GA, Curr. Med. Chem 2018, 25, 5540–5563; [PubMed: 29278205] c) Nelson JS, McCullough JL and Berns MW, J Natl Cancer Inst 1988, 80, 56–60; [PubMed: 2963136] d) Wen X, Li Y and Hamblin MR, Photodiagn. Photodyn. Ther 2017, 19, 140–152; e) Woodburn KW, Fan Q, Kessel D, Luo Y and Young SW, J. Invest. Dermatol 1998, 110, 746–751; [PubMed: 9579539] f) Davids LM and Kleemann B, Cancer Treat. Rev 2011, 37, 465–475. [PubMed: 21168280]
- [7]. Huang YY, Vecchio D, Avci P, Yin R, Garcia-Diaz M and Hamblin MR, Biol. Chem 2013, 394, 239–250. [PubMed: 23152406]
- [8]. Li J, Wang Y, Liang R, An X, Wang K, Shen G, Tu Y, Zhu J and Tao J, Nanomedicine 2015, 11, 769–794. [PubMed: 25555352]
- [9]. a) Wen X, Zhang X, Szewczyk G, El-Hussein A, Huang Y-Y, Sarna T and Hamblin MR, Antimicrob. Agents Chemother 2017, 61, e00467–00417; [PubMed: 28438946] b) Hamblin MR, Expert Rev. Anti. Infect. Ther 2017, 15, 1059–1069; [PubMed: 29084463] c) Hamblin MR, Curr. Opin. Microbiol 2016, 33, 67–73; [PubMed: 27421070] d) Vieira C, Gomes A, Mesquita MQ, Moura NMM, Neves M, Faustino MAF and Almeida A, Front. Microbiol 2018, 9, 2665. [PubMed: 30510542]
- [10]. a) Hayashi S, Ishikawa S, Ishii E, Koike M, Kaminaga T, Hamasaki Y, Sairenchi T, Kobashi G and Igawa K, J. Invest. Dermatol 2020; b) Costa RO, Macedo PM, Carvalhal A and Bernardes-Engemann AR, An. Bras. Dermatol 2013, 88, 396–402. [PubMed: 23793210]
- [11]. a) Giuntini F, Faustino MAF, Neves MGPMS, Tomé AC, Silva AMS and Cavaleiro JAS, Tetrahedron 2005, 61, 10454–10461; b) Costa LD, Guieú S, Rocha J, Silva AMS and Tomé AC, New J. Chem 2017, 41, 2186–2192.
- [12]. Castro KADF, Brancini GTP, Costa LD, Biazzoto J, Faustino MA, Tomé A, Neves MGPMS, Almeida A, Hamblin MR, da Silva RS and Braga GÚ, Photochem. Photobiol. Sci 2020, 19, 1063–1071.
- [13]. Dzieciuch M, Rissanen S, Szydłowska N, Bunker A, Kumorek M, Jamroz D, Vattulainen I, Nowakowska M, Rog T and Kepczynski M, J. Phys. Chem. B 2015, 119, 6646–6657. [PubMed: 25965670]
- [14]. Kumar S and Jain SL, Ind. Eng. Chem. Res 2014, 53, 541–546.

- [15]. a) Castro KADF, Moura NMM, Simões MMQ, Cavaleiro JAS, Faustino MAF, Cunha Â, Almeida Paz FA, Mendes RF, Almeida A, Freire CSR, Vilela C, Silvestre AJD, Nakagaki S and Neves MGPMS, *Appl. Mater. Today* 2019, 16, 332–341;b) Silva S, Pereira PMR, Silva P, Paz FAA, Faustino MAF, Cavaleiro JAS and Tomé JPC, *Chem. Commun* 2012, 48, 3608–3610;c) Mosinger J, Janošková M, Lang K and Kubát P, *Photochem J. Photobiol. A* 2006, 181, 283–289.
- [16]. a) Ding H, Sumer BD, Kessinger CW, Dong Y, Huang G, Boothman DA and Gao J, *J Control Release* 2011, 151, 271–277; [PubMed: 21232562] b) Syu WJ, Yu HP, Hsu CY, Rajan YC, Hsu YH, Chang YC, Hsieh WY, Wang CH and Lai PS, *Small* 2018, 14;c) Nascimento BFO, Pereira NAM, Valente AJM, Pinho EMT and Pineiro M, *Pharmaceutics* 2019, 11.
- [17]. Huang L, Szewczyk G, Sarna T and Hamblin MR, *ACS Infect. Dis* 2017, 3, 320–328. [PubMed: 28207234]

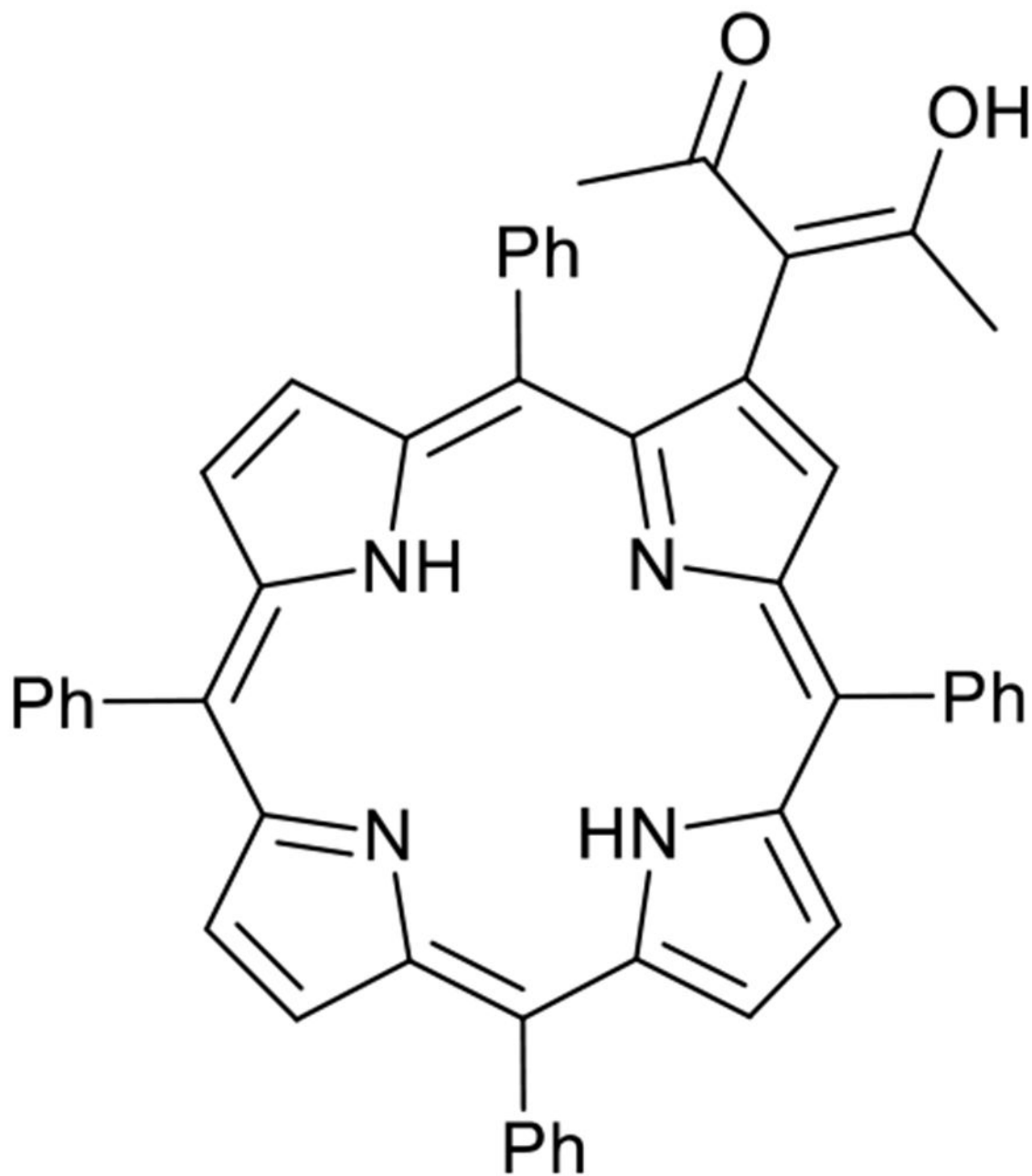


Figure 1.
Chemical structure of (1), the porphyrin used as photosensitizer in this work

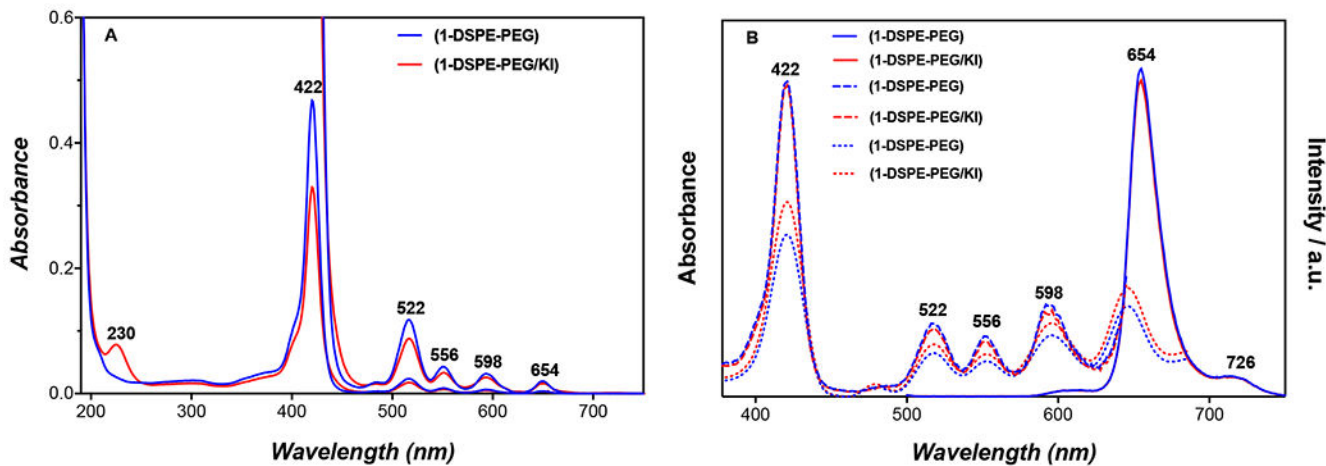


Figure 2.

Absorption, emission and excitation spectra of lipid formulations (**1-DSPE-PEG**) and (**1-DSPE-PEG/KI**) in water at concentration of 1 or 10 μM . A: Absorption spectra; B: Emission spectra (solid line), $\lambda_{\text{exc}} = 420 \text{ nm}$ and excitation spectra, $\lambda_{\text{em}} = 656 \text{ nm}$ (dash line) or 726 nm (dot line).

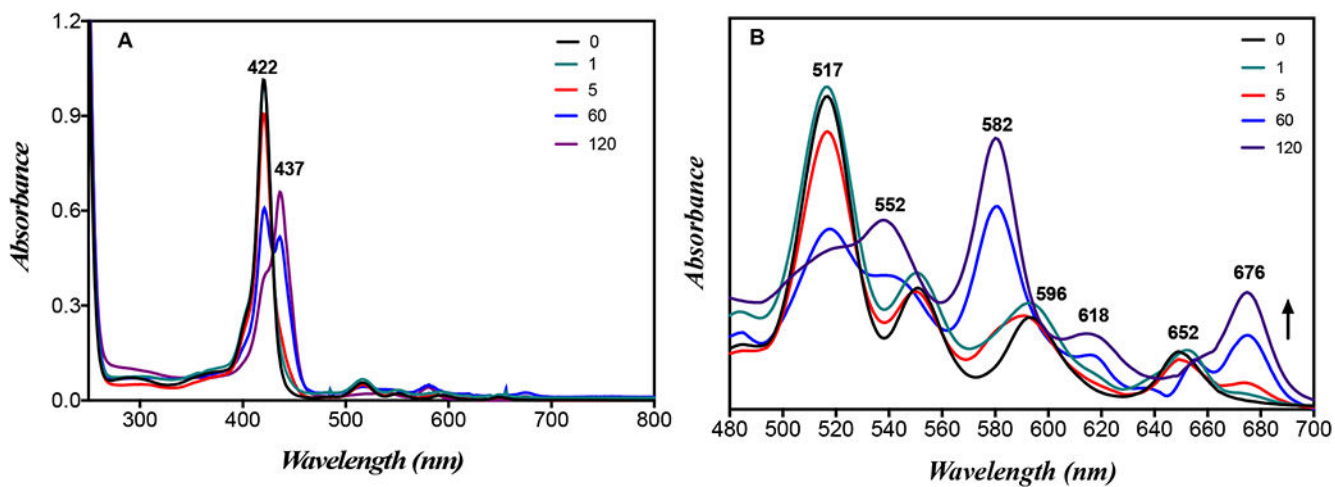


Figure 3. Absorption spectra of (1-DSPE-PEG/KI) in PBS at concentration of 2 μM before (0 min) and after 1, 5, 60 and 120 min of blue light irradiation (405 nm): (A) Soret band (B) Q-bands; the spectra for other irradiation times are shown in the SI.

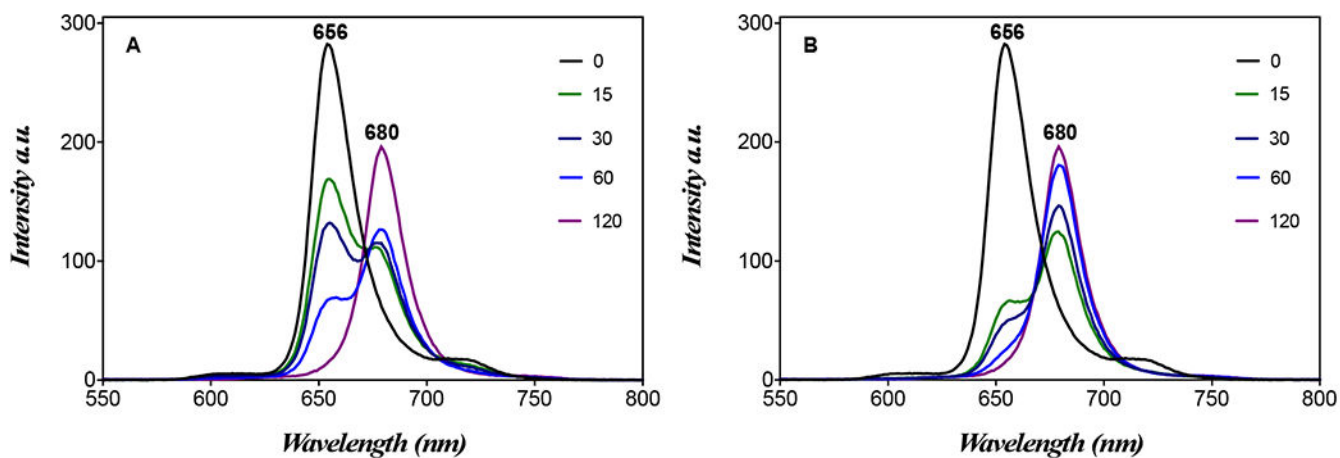


Figure 4. Emission spectra of (1-DSPE-PEG/KI) in PBS at concentration of 2 mM before (0 min) and after 15, 30, 60 and 120 min of blue light irradiation (405 nm): (A) $\lambda_{\text{exc}} = 420$ nm; (B) $\lambda_{\text{exc}} = 437$ nm at 278 K.

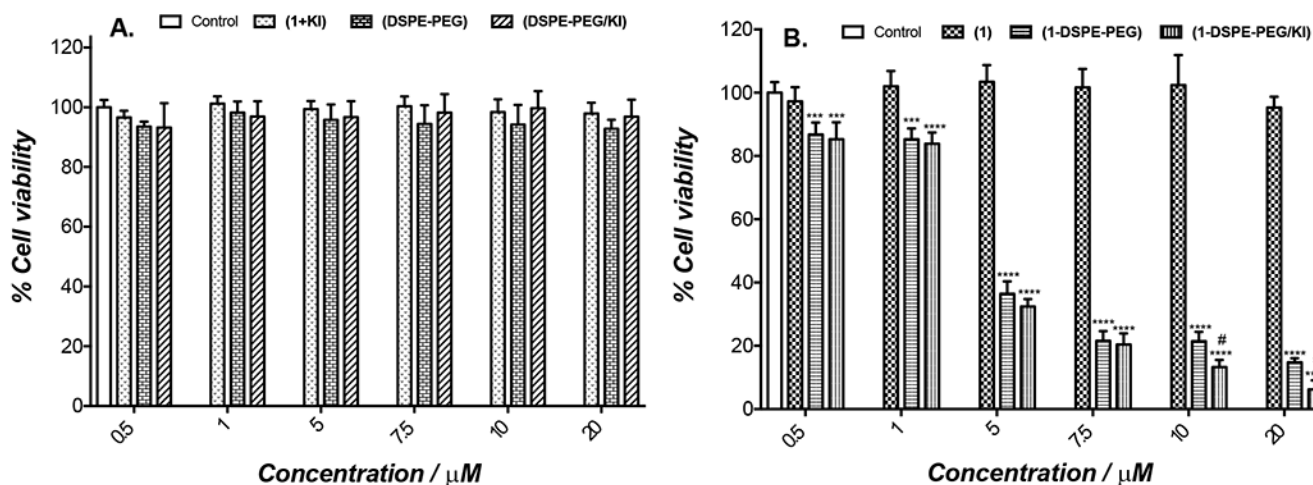


Figure 5.

Photocytotoxicity of porphyrin (**1**), porphyrin (**1**) with KI in solution (**1** + KI), lipid formulations (**1-DSPE-PEG**) and (**1-DSPE-PEG/KI**) at PS concentrations between 0.5-20 μM and lipid formulations without or with KI in the absence of (**1**) against B16F10 cancer cells determined by resazurin fluorometric assay. B16F10 cells were irradiated with blue light (405 nm) from a LED array at a total light dose of 5 J/cm^2 using different concentrations of PS. (A) (**1** + KI) and lipid formulations without (**1**) and (B) non-encapsulated porphyrin (**1**) and lipid formulations (**1-DSPE-PEG**) and (**1-DSPE-PEG/KI**). All cultures were processed under the same conditions. For (**1-DSPE-PEG/KI**), the concentration of KI is ten times the concentration of porphyrin (**1**). For the controls (**DSPE-PEG**) and (**DSPE-PEG/KI**) without (**1**), the solutions were prepared using the same volume used for preparation of (**1-DSPE-PEG**) and (**1-DSPE-PEG/KI**), respectively. In the experiments performed using only KI solution, no significant reduction in cell viability with or without irradiation was observed. The results are presented as mean \pm standard deviation of three independent experiments performed in triplicate. Significant differences relative to control cell cultures are presented with an *. Statistical significance: *** $p < .001$ and **** $p < .0001$ and with # the significant differences with respect to (**1-DSPE-PEG**).

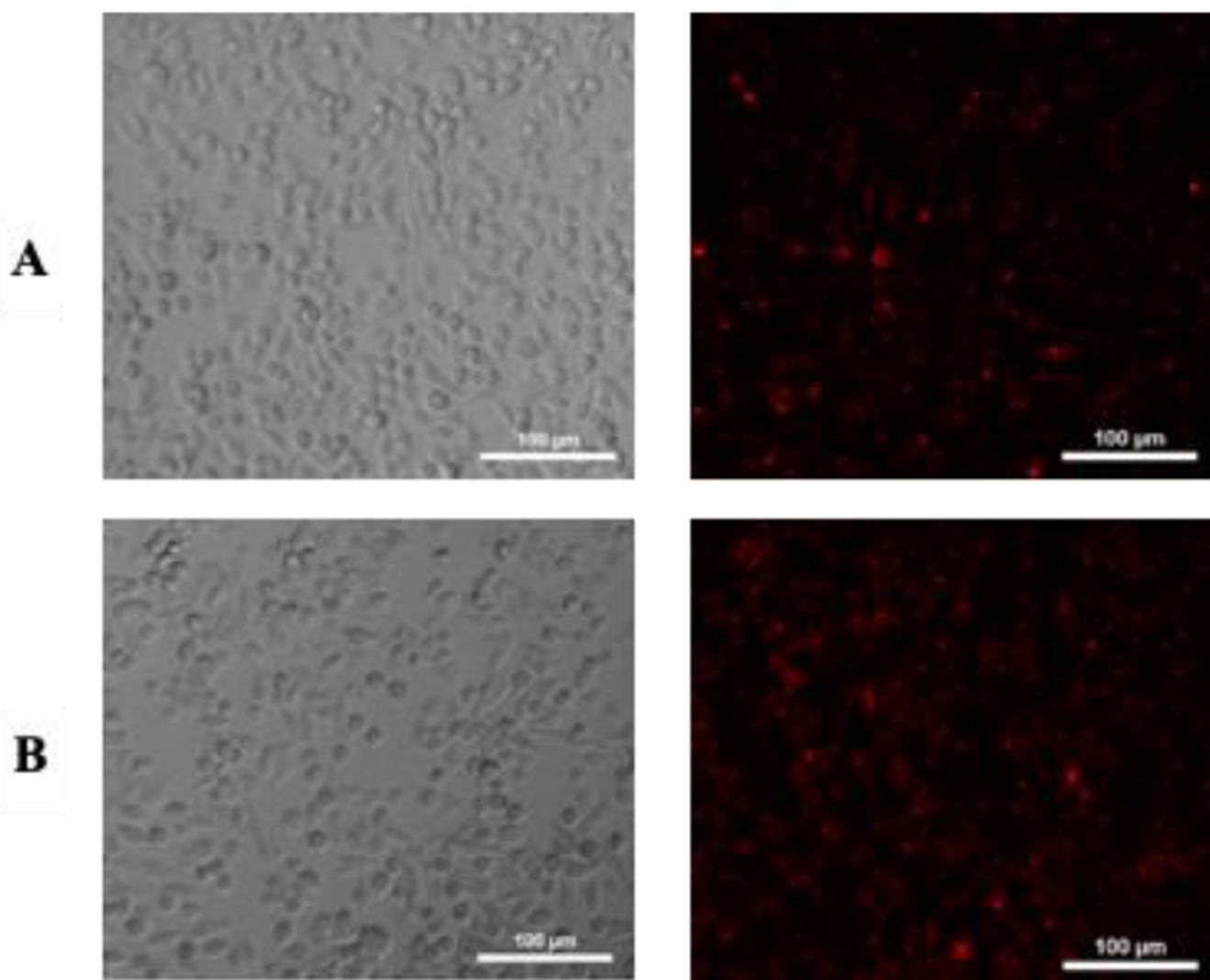


Figure 6. Internalization of lipid formulations by B16F10 cells determined by fluorescence microscopy. From the left to right: Bright field and lipid formulations internalized. A) images of B16F10 cells treated with (1-DSPE-PEG) and B) (1-DSPE-PEG/KI), respectively, after 4 h of incubation.